

Bias-controlled sensitivity of ferromagnet/semiconductor electrical spin detectors

S. A. Crooker,^{1,*} E. S. Garlid,² A. N. Chantis,¹ D. L. Smith,¹ K. S. M. Reddy,³ Q. O. Hu,² T. Kondo,^{2,†} C. J. Palmström,^{3,4} and P. A. Crowell²

¹*Los Alamos National Laboratory, Los Alamos, New Mexico 87545, USA*

²*School of Physics and Astronomy, University of Minnesota, Minneapolis, Minnesota 55455, USA*

³*Department of Chemical Engineering & Materials Science, University of Minnesota, Minneapolis, Minnesota 55455, USA*

⁴*Departments of Electrical & Computer Engineering and Materials, University of California, Santa Barbara, California 93106, USA*
(Received 9 June 2009; published 10 July 2009)

Using Fe/GaAs Schottky tunnel barriers as electrical spin detectors, we show that the magnitude and the sign of their spin-detection sensitivities can be widely tuned with the voltage bias applied across the Fe/GaAs interface. Experiments and theory establish that this tunability derives not just simply from the bias dependence of the tunneling conductances $G_{\uparrow,\downarrow}$ (a property of the interface), but also from the bias dependence of electric fields in the semiconductor which can dramatically enhance or suppress spin-detection sensitivities. Electrons in GaAs with fixed polarization can therefore be made to induce either positive or negative voltage changes at spin detectors, and some detector sensitivities can be enhanced over tenfold compared to the usual case of zero-bias spin detection.

DOI: 10.1103/PhysRevB.80.041305

PACS number(s): 72.25.Dc, 72.25.Hg, 72.25.Mk, 85.75.-d

An all-electrical scheme for efficient detection of spins is an essential component of most “semiconductor spintronic” device proposals,^{1,2} and recent demonstrations of electrical spin injection and detection in GaAs,^{3–5} silicon,^{6,7} and graphene⁸ have motivated a desire to understand how bulk and interfacial spin transport contribute to device performance. However, while the need for optimizing spin injection is widely recognized, the interplay among mechanisms that govern electrical spin detection has only begun to be explored.^{2,4,9}

Recent progress on spin-transport devices with semiconductor channels has relied on spin-dependent electron tunneling through barriers formed at ferromagnet-semiconductor interfaces.^{10–12} However, tunneling typically introduces a strong and often unpredictable dependence of the tunneling current polarization P_j on interface voltage bias. For example, tunneling magnetoresistances through vertical Fe/GaAs/Fe trilayers were found to invert sign when one interface was epitaxial.¹³ In lateral Fe/GaAs devices, P_j varied markedly with source electrode bias, unexpectedly inverting sign under forward bias in some structures and under reverse bias in others.⁵ Accordingly, several recent theories have attempted to understand spin tunneling through ferromagnet-semiconductor interfaces.^{9,14,15} In addressing the relevance of these models to the equally important problem of spin detection, there is a critical and largely unexplored need to separate interfacial tunneling effects from the effects of spin transport due to electric fields^{16,17} in the semiconductor.

Here we use lateral Fe/GaAs structures to study the influence of a detector interface bias (V_d) on the sensitivity of electrical spin detection, which we define as the voltage change ΔV_d induced by an additional remotely injected spin polarization. Crucially, we show that spin-detection sensitivities cannot be understood from the detector interface’s tunneling properties (P_j) alone. Instead, both experiments and theory show that ΔV_d can be *significantly* enhanced or suppressed compared to P_j —in a controlled and predictable fashion—due to the resulting electric fields in the semiconductor, which modify the spin densities ($n_{\uparrow,\downarrow}$) and their gradients at biased Fe/GaAs detector interfaces. These new phe-

nomena cannot occur in conventional nonlocal studies that use spin detectors operating at zero bias, nor are they expected in all-metal devices having large channel conductivities and therefore negligible electric fields.

Figure 1(a) shows a typical device. Epitaxial Fe/GaAs structures are processed into lateral spin-transport devices having five $10 \times 50 \mu\text{m}^2$ Fe contacts (Nos. 1–5) on a $2.5\text{-}\mu\text{m}$ -thick n -type GaAs channel.⁵ A Schottky tunnel barrier is formed at the interface between Fe and a highly doped n^+ interfacial layer of GaAs.¹⁸ Devices from two wafers are discussed (denoted A and B, with $n=3.5$ and $2.0 \times 10^{16} \text{ cm}^{-3}$); these represent structures for which P_j inverts under finite forward and reverse source biases, respectively.⁵

To measure the spin-detection sensitivity of these Fe/GaAs electrodes in a background-free manner, we employ an optical pumping technique. First, a constant current j establishes a voltage drop V_d across a Fe/GaAs detector interface (contact 4 in Fig. 1). From Ref. 12,

$$V_d = \frac{j}{4} \left[\left(\frac{1}{G_{\uparrow}} + \frac{1}{G_{\downarrow}} \right) + \left(\frac{1}{G_{\uparrow}} - \frac{1}{G_{\downarrow}} \right) P_j \right], \quad (1)$$

where $P_j = (j_{\uparrow} - j_{\downarrow})/j$ is the tunneling current polarization and $j_{\uparrow,\downarrow}$ and $G_{\uparrow,\downarrow}$ are the majority- and the minority-spin tunneling currents and conductances. A weak, circularly polarized 1.58 eV pump laser is then focused to a stripe $10\text{--}20 \mu\text{m}$ away from contact 4, injecting a small constant spin polarization in the channel. This additional polarization, oriented initially along $\pm \hat{z}$, drifts and diffuses laterally and is tipped into the minority- or the majority-spin direction with respect to the Fe magnetization \mathbf{M} ($\parallel \pm \hat{y}$) by small applied fields $\pm B_x$. At the Fe/GaAs detector interface, this polarization modifies the chemical potentials $\mu_{\uparrow,\downarrow}$, which (at constant j) necessarily modifies P_j and therefore changes V_d by an amount ΔV_d that is a direct measure of the detector’s spin sensitivity. The dependence of ΔV_d on V_d derives both from the bias dependence of $G_{\uparrow,\downarrow}$ (a property of the interface) and

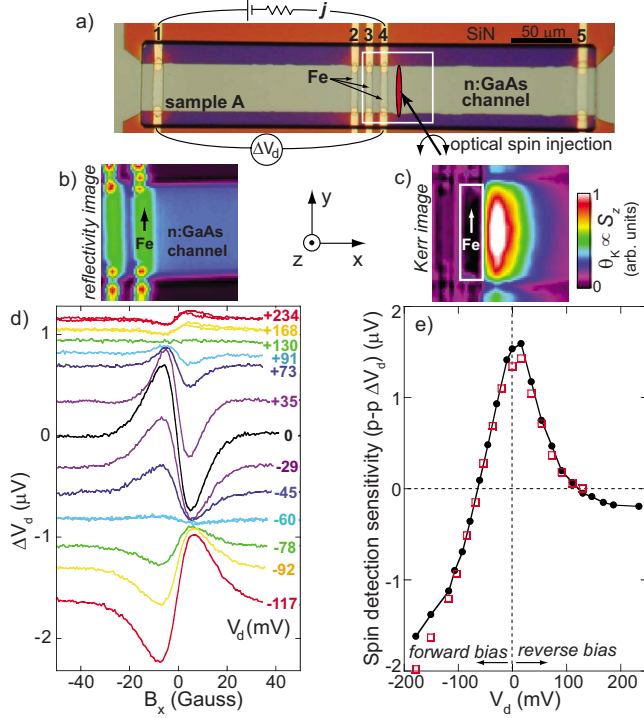


FIG. 1. (Color online) (a) Spin-transport device A and the spin-detection experiment. Current j establishes a voltage V_d across a Fe/GaAs detector interface (contact 4). Changes (ΔV_d) due to a remotely optically injected spin polarization reveal the detector's spin sensitivity. (b) A $70 \times 70 \mu\text{m}^2$ reflectivity image [white square in (a)], showing device features. (c) A Kerr-rotation image of the optically injected polarization ($B_x = 0$). (d) Raw spin-detection data at 10 K, $\Delta V_d(B_x)$, at various V_d . 4 and 20 K data are very similar. (e) The corresponding spin-detection sensitivity versus V_d (black points). Squares show similar ΔV_d measured for injection in the current path (j flowing between contacts 4 and 5).

from the optically induced changes to P_j (which depends on electric fields in the GaAs, as detailed later).

To explicitly measure spin-dependent changes, the laser is modulated from right- to left-circular polarization at 50 kHz, and ΔV_d at this frequency is measured between the detector and a distant reference contact. Importantly, this approach avoids magnetic dichroism and hot electron artifacts because spins are injected into the channel (rather than through the Fe contact), where they cool before diffusing. Using scanning Kerr-rotation microscopy,^{19–22} Figs. 1(b) and 1(c) show images of the reflectivity and of the optically injected polarization diffusing to the right and also to the left toward the spin detector. Using low laser power ($\sim 10 \mu\text{W}$), perturbations to $\mu_{\uparrow,\downarrow}$ are intentionally kept small, of order $1 \mu\text{V}$.

Figure 1(d) shows ΔV_d versus B_x at different biases V_d across the Fe/GaAs detector. Effectively, we electrically detect the \hat{y} component of diffusing and precessing spins that are optically oriented initially along $\pm \hat{z}$. Thus, the data show antisymmetric “local Hanle” line shapes that depend on spin lifetimes, diffusion constants, and source/detector separation.^{20,21} Maximum and minimum ΔV_d occur at $\pm B_x$ for which the injected spins precess on average $\pm 90^\circ$ ($\parallel \pm \mathbf{M}$) upon reaching the detector. Larger B_x causes rapid ensemble dephasing.

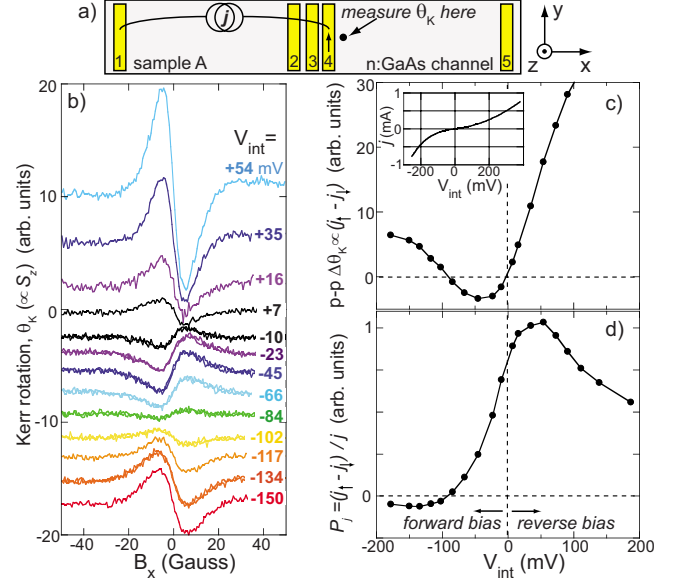


FIG. 2. (Color online) (a) Measuring P_j , the tunneling current polarization at contact 4 via spin injection at 10 K. Current j establishes a voltage bias V_{int} across the Fe/GaAs interface. (b) Electrically injected spins are measured via the Hanle-Kerr effect (θ_K vs B_x), at different V_{int} (curves offset). (c) The peak-to-peak Hanle amplitude, $\Delta \theta_K \propto j_{\uparrow} - j_{\downarrow}$, versus V_{int} . Inset: $j(V_{int})$ for contact 4. (d) Relative polarization, $P_j \propto (j_{\uparrow} - j_{\downarrow})/j$, versus V_{int} .

The peak-to-peak amplitudes of these curves [Fig. 1(e)] therefore provide a relative measure of the electrical spin-detection sensitivity that depends only on the spin-dependent voltages induced by the remotely injected spins. In sample A, ΔV_d is clearly tunable with the detector bias. It is large and positive near $V_d = 0$, where the remotely injected spins induce a positive ΔV_d ($\approx +1.5 \mu\text{V}$) at the detection electrode. With increasing forward or reverse detector bias, however, ΔV_d decreases and inverts sign—now, these same spins induce a *negative* voltage change. Electrons in GaAs with fixed spin can therefore be made to generate positive *or* negative voltage changes at these Fe/GaAs spin detectors by tuning V_d by a few tens of mV, offering new routes (besides manipulating electron spins or contact magnetizations) to tune and switch spin-dependent electrical signals.

To understand this tunable spin-detection sensitivity, it is essential to independently measure P_j , the polarization of the tunneling current that flows across this biased Fe/GaAs interface. For this we measure the electrical spin *injection* efficiency of this electrode using Kerr-rotation methods, as demonstrated previously.⁵ Here (see Fig. 2), a probe laser detects the \hat{z} component of electrically injected spins via the Hanle-Kerr effect, θ_K versus B_x , at a point $\sim 10 \mu\text{m}$ to the right of contact 4. These $\theta_K(B_x)$ curves exhibit similar local Hanle line shapes as seen in Fig. 1(d). Extrema occur at $\pm B_x$ for which the spins have on average precessed $\pm 90^\circ$ (from $\pm \hat{y}$ to $\pm \hat{z}$) at the detection point. A series of curves are shown in Fig. 2(b) at various interface biases V_{int} across contact 4. Their peak-to-peak amplitude $\Delta \theta_K$ is proportional to the difference between injected majority- and minority-spin densities, which necessarily scales directly with the difference between majority- and minority-spin tunneling cur-

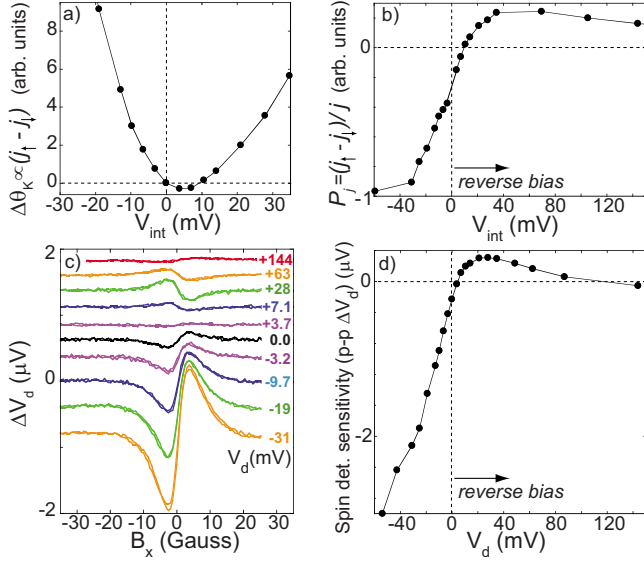


FIG. 3. (Color online) Spin injection and detection data from sample B at 10 K. (a) The electrically injected spin density, measured by the Kerr effect ($\Delta\theta_K$ vs V_{int}). (b) Polarization of the tunneling current P_j , which now inverts under *reverse* bias, in contrast to sample A. (c) Raw spin-detection data, $\Delta V_d(B_x)$ at various detector biases V_d (curves offset). (d) The spin-detection sensitivity ΔV_d versus V_d .

rents: $\Delta\theta_K \propto n_{\uparrow} - n_{\downarrow} \propto j_{\uparrow} - j_{\downarrow}$. Figure 2(c) shows $\Delta\theta_K(V_{int})$ and the current-voltage trace for contact 4. Normalizing by the total current j reveals the relative polarization of the interface tunneling current, $P_j \propto (j_{\uparrow} - j_{\downarrow})/j$ [see Fig. 2(d)]. P_j depends strongly on V_{int} , showing a maximum (majority spin) polarization near +50 mV and a sign inversion at -90 mV forward bias. All contacts on sample A and on other devices from this wafer show the same bias dependence of P_j .

Comparing sample A's spin-detection sensitivity ΔV_d with P_j [Figs. 1(e) and 2(d)], general trends can now be identified: both exhibit a positive maximum near zero bias, and the inversion of ΔV_d under small forward bias can now be understood by the similar inversion of P_j . However, a key finding is that striking differences exist at large interface bias: compared to P_j , $|\Delta V_d|$ is markedly *enhanced* under large forward bias but is *suppressed* under large reverse bias (ΔV_d also inverts sign again at +130 mV, which is unexpected and does not follow from P_j). Thus, spin-detection sensitivities in these Fe/GaAs structures do *not* simply track P_j as might be expected from reciprocity arguments, and their strong deviation at larger biases suggests the important and nontrivial role of electric fields in the GaAs, as discussed below.

Figure 3 shows corroborating data from sample B. In contrast to sample A, injection studies [Figs. 3(a) and 3(b)] show that P_j is now dominated by *minority* spins at zero bias and that P_j now inverts at finite *reverse* bias ($\sim +10$ mV). These differences likely originate in the microscopic details of this Fe/GaAs interface, which are not yet fully understood.^{14,15} Nonetheless, the sensitivity of sample B's spin detectors [Figs. 3(c) and 3(d)] can be correlated with P_j . At zero bias, the remotely injected spins now generate small *negative* voltage changes at detection electrodes ($\Delta V_d \approx -0.2$ μ V), which now invert sign at small reverse detector bias, similar to P_j .

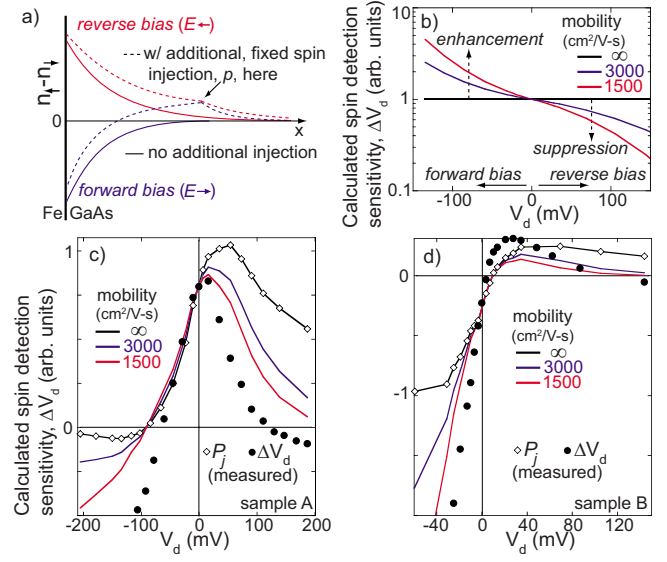


FIG. 4. (Color online) (a) Schematic of $n_{\uparrow} - n_{\downarrow}$ near a Fe/GaAs spin detector under forward or reverse bias V_d (solid lines). Both $n_{\uparrow} - n_{\downarrow}$ and its gradient are modified (dashed lines) by a remotely injected polarization p . (b) Calculated sensitivity of a spin detector having *constant* P_j . Enhancement and suppression are due to E fields in the GaAs. [(c),(d)] Calculated ΔV_d for samples A and B, for three electron mobilities μ , using measured P_j (open symbols) as inputs and p injected 20 μ m away.

However, like sample A, ΔV_d diverges markedly from P_j at large bias: ΔV_d is suppressed at large reverse bias but is greatly enhanced—over tenfold—with only -40 mV forward bias, transforming a poor zero-bias spin detector into a much more sensitive spin-detection device.

The enhancement and the suppression of ΔV_d can be understood within a one-dimensional (1D) model of spin transport in the semiconductor and its nontrivial influence on spin detection.²³ As Fig. 4(a) depicts, a unit polarization p generated in the channel modifies the spin-density difference $n_{\uparrow} - n_{\downarrow}$ and its gradient at a nearby Fe/GaAs detector interface (in the figure, both increase). At a fixed interface current j , these modifications necessarily change P_j if $G_{\uparrow} \neq G_{\downarrow}$. From Eq. (1), one can derive the induced change in detector voltage: $\Delta V_d \propto k \frac{\partial P_j}{\partial p} = k \left\{ D \frac{\partial}{\partial p} \left[\frac{\partial (n_{\uparrow} - n_{\downarrow})}{\partial x} \right] + \mu E \frac{\partial}{\partial p} (n_{\uparrow} - n_{\downarrow}) \right\}$, where $k = \frac{e}{4} \left(\frac{1}{G_{\uparrow}} - \frac{1}{G_{\downarrow}} \right)$, D and μ are the electron diffusion constant and the mobility, E is the electric field in the semiconductor, and $n_{\uparrow} - n_{\downarrow}$ and its gradient are evaluated at the interface. Using the spin-transport model of Ref. 12 and the full spin-drift-diffusion equations, one finds²³ that ΔV_d can deviate markedly from P_j because: (i) trivially, E can drift p away from (toward) the detector in reverse (forward) bias, while (ii) *at the interface itself*, the diffusion and the drift terms oppose each other in reverse bias ($E < 0$) but add in forward bias ($E > 0$). The importance of (ii) is clearly seen in Fig. 1(e), where nearly identical detection sensitivities are measured even when p is injected *in* the current path. Note that $|E| < 10$ V/cm, rather modest, in these studies.

These enhancement and suppression effects are normally superimposed on the bias dependence of P_j but are disentangled in Fig. 4(b) by showing ΔV_d calculated for an ideal-

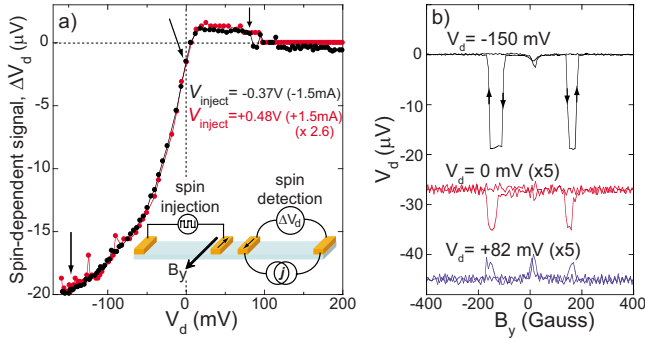


FIG. 5. (Color online) (a) Inset: all-electrical lateral spin-valve setup. Black (red/gray) points show the spin-valve signal ΔV_d versus detector bias V_d for a forward (reverse) biased spin injector. (b) Raw spin-valve data at three detector biases [arrows in (a)], using a fixed -1.5 mA injector bias (curves offset). Note sign switching and tenfold enhancement of the detected signal.

ized (constant) P_j . Crucially, detection sensitivities are enhanced or suppressed relative to P_j due to E , which depends sensitively on the channel conductivity. For “metallic-like” channels, ΔV_d tracks P_j exactly, because $E \sim 0$. Notably, this model suggests that ΔV_d can also be controlled (independent of P_j) by engineering the conductivity of semiconductor devices.

We explicitly calculate ΔV_d for samples A and B using $G_{\uparrow,\downarrow}$ determined from experimental P_j and $j(V_{int})$ data. Electron densities and spin lifetimes are measured independently. The results [Figs. 4(c) and 4(d)] are scaled, so that $\Delta V_d \equiv P_j$ at zero bias. For realistic n :GaAs mobilities, the

calculated $|\Delta V_d|$ drops (increases) much more rapidly than P_j under large reverse (forward) bias, in good overall agreement with measured ΔV_d values. (The inversion of ΔV_d at large reverse bias is not reproduced in this 1D model because drift and diffusion terms cancel exactly, suppressing ΔV_d monotonically to zero.²³ No such restriction exists in two- or three-dimensional geometries, which permit inhomogeneous E fields.)

Finally, these results suggest that it should be possible to tune and enhance the detection of *electrically* injected spins. This is demonstrated in Fig. 5, where nonlocal lateral spin-valve studies⁵ were performed on a device having P_j similar to sample B. Figure 5(a) shows the spin-valve signal versus the detector bias, when the *source* electrode is forward or reverse biased. The dependence on V_d is the same, confirming that a detector’s sensitivity can be optimized independently of an injector’s biasing. Figure 5(b) shows raw spin-valve data with $V_d = -150$, 0, and $+82$ mV, explicitly showing that spin-detection sensitivities are freely tunable in both sign and magnitude in all-electrical devices.

In these studies, both interfacial biases and electric fields play essential roles. Because semiconductors can support large electric fields, it is possible to bias each element—source, channel, and detector—independently. Controlling spin transport through both interfacial and bulk band structures represents a unique capability of ferromagnet-semiconductor devices that is only beginning to be explored.

The authors acknowledge the support from the Los Alamos LDRD program, ONR, NSF MRSEC, NNIN, IGERT programs, and the Japan Society for the Promotion of Science.

*crooker@lanl.gov

[†]On leave from the Imaging Science and Engineering Laboratory, Tokyo Institute of Technology, Yokohama 226, Japan.

¹I. Žutić, J. Fabian, and S. Das Sarma, Rev. Mod. Phys. **76**, 323 (2004).

²R. Jansen and B. C. Min, Phys. Rev. Lett. **99**, 246604 (2007).

³P. R. Hammar and M. Johnson, Phys. Rev. Lett. **88**, 066806 (2002).

⁴D. Saha, M. Holub, and P. Bhattacharya, Appl. Phys. Lett. **91**, 072513 (2007).

⁵X. Lou, C. Adelman, S. A. Crooker, E. S. Garlid, J. Zhang, K. S. M. Reddy, S. D. Flexner, C. J. Palmstrøm, and P. A. Crowell, Nat. Phys. **3**, 197 (2007).

⁶I. Appelbaum, B. Huang, and D. J. Monsma, Nature (London) **447**, 295 (2007).

⁷O. M. J. van ’t Erve, A. T. Hanbicki, M. Holub, C. H. Li, C. Awo-Affouda, P. E. Thompson, and B. T. Jonker, Appl. Phys. Lett. **91**, 212109 (2007).

⁸N. Tombros, C. Jozsa, M. Popinciuc, H. T. Jonkman, and B. J. van Wees, Nature (London) **448**, 571 (2007).

⁹M. Tran, H. Jaffrès, C. Deranlot, J.-M. George, A. Fert, A. Miar, and A. Lemaître, Phys. Rev. Lett. **102**, 036601 (2009).

¹⁰M. Johnson and R. H. Silsbee, Phys. Rev. Lett. **60**, 377 (1988).

¹¹E. I. Rashba, Phys. Rev. B **62**, R16267 (2000).

¹²D. L. Smith and R. N. Silver, Phys. Rev. B **64**, 045323 (2001).

¹³J. Moser, M. Zenger, C. Gerl, D. Schuh, R. Meier, P. Chen, G.

Bayreuther, W. Wegscheider, D. Weiss, C.-H. Lai, R.-T. Huang, M. Kosuth, and H. Ebert, Appl. Phys. Lett. **89**, 162106 (2006).

¹⁴H. Dery and L. J. Sham, Phys. Rev. Lett. **98**, 046602 (2007).

¹⁵A. N. Chantis, K. D. Belashchenko, D. L. Smith, E. Y. Tsybal, M. van Schilfgaarde, and R. C. Albers, Phys. Rev. Lett. **99**, 196603 (2007).

¹⁶Z. G. Yu and M. E. Flatté, Phys. Rev. B **66**, 201202(R) (2002).

¹⁷G. Schmidt, C. Gould, P. Grabs, A. M. Lunde, G. Richter, A. Slobodskyy, and L. W. Molenkamp, Phys. Rev. Lett. **92**, 226602 (2004).

¹⁸A. T. Hanbicki, O. M. J. van ’t Erve, R. Magno, G. Kioseoglou, C. H. Li, B. T. Jonker, G. Itkos, R. Mallory, M. Yasar, and A. Petrou, Appl. Phys. Lett. **82**, 4092 (2003).

¹⁹J. Stephens, J. Berezovsky, J. P. McGuire, L. J. Sham, A. C. Gossard, and D. D. Awschalom, Phys. Rev. Lett. **93**, 097602 (2004).

²⁰S. A. Crooker, M. Furis, X. Lou, C. Adelman, D. L. Smith, C. J. Palmstrøm, and P. A. Crowell, Science **309**, 2191 (2005).

²¹M. Furis, D. L. Smith, S. Kos, E. S. Garlid, K. S. M. Reddy, C. J. Palmstrøm, P. A. Crowell, and S. A. Crooker, New J. Phys. **9**, 347 (2007).

²²P. Kotissek, M. Bailleul, M. Sperl, A. Spitzer, D. Schuh, W. Wegscheider, C. H. Back, and G. Bayreuther, Nat. Phys. **3**, 872 (2007).

²³A. N. Chantis and D. L. Smith, Phys. Rev. B **78**, 235317 (2008).